

RSC Advances



This is an *Accepted Manuscript*, which has been through the Royal Society of Chemistry peer review process and has been accepted for publication.

Accepted Manuscripts are published online shortly after acceptance, before technical editing, formatting and proof reading. Using this free service, authors can make their results available to the community, in citable form, before we publish the edited article. This *Accepted Manuscript* will be replaced by the edited, formatted and paginated article as soon as this is available.

You can find more information about *Accepted Manuscripts* in the [Information for Authors](#).

Please note that technical editing may introduce minor changes to the text and/or graphics, which may alter content. The journal's standard [Terms & Conditions](#) and the [Ethical guidelines](#) still apply. In no event shall the Royal Society of Chemistry be held responsible for any errors or omissions in this *Accepted Manuscript* or any consequences arising from the use of any information it contains.

Electronic structure and optical properties of Si-O-N compounds on different crystal structures

Zhi-Gang Duan,^{1,3} Zong-Yan Zhao,^{1,*} Pei-Zhi Yang,^{2,*}

¹ Faculty of Materials Science and Engineering, Key Laboratory of Advanced Materials of Yunnan Province, Kunming University of Science and Technology, Kunming 650093, People's Republic of China

² Key Laboratory of Advanced Technique & Preparation for Renewable Energy Materials, Ministry of Education, Yunnan Normal University, Kunming 650092, People's Republic of China

³ College of Science, Southwest Forestry University, Kunming 650224, People's Republic of China

* E-mail: zzy@kmust.edu.cn (Z. Zhao); pzhyang@hotmail.com (P. Yang). Tel: +86-871-65109952, Fax: +86-871-65107922.

Abstract

In order to explore the relationship between crystal structure and optical properties, five Si-O-N compounds in different crystal structures, including: α -quartz SiO_2 , β -quartz SiO_2 , $\text{Si}_2\text{N}_2\text{O}$, α - Si_3N_4 , β - Si_3N_4 were considered in the present work. Using density functional theory with GGA+U method, their crystal structure, electronic structure, and optical properties have been systematically investigated. The electronic structure of α and β phases of SiO_2 (or Si_3N_4) are similar, but with some subtle differences than can be attributed to the different local bonding structure. And the electronic structure of $\text{Si}_2\text{N}_2\text{O}$ gathers the fundamental features of electronic properties of SiO_2 and Si_3N_4 . Based on the calculated results, it is found that the optical properties not only are determined by the component of Si-O-N compounds, but also are determined by the microstructure of Si-O-N compounds. These calculated results will be useful as reference data for analyzing the optical properties of more complicated SiO_xN_y compounds. According to this principle, one could design novel Si-O-N compounds for specific optoelectronic applications, via tuning the composition and crystal structure.

Keywords

Si-O-N compounds; Electronic structure; Optical properties; DFT calculations

1. Introduction

Silicon-nitrogen-oxygen compounds, including: silicon dioxide (silica, SiO_2), silicon nitride (Si_3N_4), silicon oxynitride ($\text{Si}_2\text{N}_2\text{O}$), SiO_xN_y , etc., are important versatile functional materials. SiO_2 is most commonly found in nature as quartz, and its applications range from structural materials to microelectronics to components used in the food industry (for example, ceramic, glass, optical fiber, refractory material, and so on). Owing to its several advantages: small linear expansion coefficient, good thermal shock resistance, low dielectric constant or thermal conductivity, simple production process, and low-cost, SiO_2 becomes more and more very important material for current electronic industry.¹ Si_3N_4 is high strength material (especially, the hot pressed Si_3N_4 is one of the world's hardest materials). Its strength can be maintained at the high temperature of 1200 °C without declining. At the same time, it has amazing resistance to chemical corrosion, and is a kind of high performance electrical insulating materials. During the past years, most of the considerable development work on Si_3N_4 has been conducted, primarily by the ceramics and electronic communities.² $\text{Si}_2\text{N}_2\text{O}$ is a stable compound in the Si_3N_4 - SiO_2 system, which has the transition structure between Si_3N_4 and SiO_2 . It is a strong covalent compound with a low density, high hardness, and has the advantages of thermal shock resistance, antioxidant, and thermodynamic stability. Thus, $\text{Si}_2\text{N}_2\text{O}$ is a kind of very promising high-temperature structural material.³ SiO_xN_y is a very important material for optoelectronic applications, owing to the possibility of tailoring its electronic structure and optical properties by its elemental composition.^{4,5} For example, the amorphous thermal gate silicon dioxide (SiO_2) should be replaced by amorphous SiO_xN_y to meet the challenge of nanoscale MOS devices, in which the gate dielectric thickness will be further scaled down to less than 4 nm.⁶

SiO_xN_y compound with excellent properties of both SiO_2 and Si_3N_4 compounds, has received the extensive concern. As a kind of similar to the valence bond structure of Si_3N_4 compound, SiO_xN_y processes particular chemical bond diversity and structural diversity, which determines its unique mechanics and thermodynamics properties of mechanics and thermodynamics (including: low density, high hardness, low thermal expansion coefficient, etc.). At high temperature of 1600 °C, SiO_xN_y still maintained good antioxidation properties. And, at high temperature of 1400 °C, its bending strength will not be significantly reduced. In recent years, SiO_xN_y film has been an important application in the field of microelectronics, is expected to replace thermal oxidation of SiO_2 as the gate material, which can improve the dielectric constant, the ability to prevent the impurity diffusion, and radiation resistance.⁷ At the same time, SiO_xN_y

thin films were also studied in the field of integrated optics. The refractive index and the extinction coefficient of SiO_xN_y thin films could be tuned by changing component proportion, resulting in applications of optical waveguide materials,^{8, 9} gradient index thin films,¹⁰ and antireflection film. This character provides more facility for the integrated optical design. In addition, SiO_xN_y thin films can be used as silicon based light emitting materials.¹¹

In the applications of solar cells, photodetectors, and photodiodes, the light trapping capability is one of the critical issues to improve the optoelectronic performance.^{12, 13} In order to enhance the light trapping capability, researchers used SiO_xN_y thin films as anti-reflective coating on the front side of the devices to reduce the light reflectance. Compared with SiO_2 component, the nitrogen component could change the dielectric constant of SiO_xN_y compound, because of the variation of the ionic polarizability.¹⁴ Recently, Qiu et al. proposed and fabricated quasi gradient index distribution of amorphous Si, SiN_x , SiO_xN_y , and SiO_2 stacks by plasma enhanced chemical vapor deposition and got a low average reflectance of 2%-4.3% from 280-3300 nm wavelength.^{4, 15} In fact, these optoelectronic applications are determined by its optical properties, such as dielectric function, refractive index, reflectivity, and so on. SiO_xN_y could break the dielectric breakdown of SiO_2 layers of 1-2 nm thickness, at the same time preserve the excellent features (high thermal stability and high electron mobility) of SiO_2 .^{16, 17} SiO_xN_y is transparent in the visible-light range and its refractive index can be varied from one of the SiO_2 (~1.44) to that of Si_3N_4 (~2.02) by only acting on the oxygen and nitrogen concentrations, as well as its band gap could be increased by increasing the oxygen amount.^{7, 18} Rebib et al. obtained SiO_xN_y layers with a large stoichiometry variation by the sputtering process of a pure silicon target under argon-oxygen-nitrogen atmosphere, and found that the refractive index of SiO_xN_y decrease linearly from 1.94 to 1.46 when the composition varies between Si_3N_4 and SiO_2 .^{19, 20}

Although, there are a lot of published works concerned the composition, properties, and performance of SiO_xN_y compounds. However, the most important aspects about the fundamental properties transition from SiO_2 , to $\text{Si}_2\text{N}_2\text{O}$, to SiO_xN_y , and to Si_3N_4 , are still lacking at present. In order to further improve the fundamental understanding of SiO_xN_y compound, and provide helpful information about the relationship between electronic structure and optical properties, we chosen five crystal structures of Si-O-N compounds (including: α -quartz SiO_2 , β -quartz SiO_2 , $\text{Si}_2\text{N}_2\text{O}$, α - Si_3N_4 , β - Si_3N_4) as research object, and adopted density functional theory (DFT) calculations as research method to investigate their electronic structure and optical properties, in the present work. These calculated results will be useful as reference data for analyzing the

optical properties of more complicated SiO_xN_y compounds.

2. Computational methods

In the present work, all of the calculations were carried out by using the periodic density functional theory package of Cambridge Serial Total Energy Package (CASTEP) codes.²¹ CASTEP is a state-of-the-art quantum mechanics-based program designed specifically for solid-state materials science. The core electrons (Si: [Ne], O: [He], N: [He]) were treated with the ultrasoft pseudopotential. The exchange-correlation effects of valence electrons (Si: $3s^23p^2$, O: $2s^22p^4$, N: $2s^22p^3$) were described by the revised Perdew-Burke-Ernzerhof for solid (PBEsol) of generalized gradient approximation (GGA).²² In order to obtain accurate electronic structure, the method of GGA+U was adopted to overcome the well-known shortcoming of GGA method.²³ The Hubbard model is one of the most successful models to describe the correlated electrons in solids. In the present work, the U value of Si (O, and N)-p orbital was set as follows: $U_{\text{eff}} = U - J = 7.90$ eV, which is obtained by comparing the theoretical calculated and experimental measured band gap of crystal α -quartz SiO_2 . The Monkhorst-Pack scheme K-points grid sampling was set as $4 \times 4 \times 2$ for the irreducible Brillouin zone. A $60 \times 60 \times 80$ mesh was used for fast Fourier transformation. An energy cutoff of 380 eV was used for expanding the Kohn-Sham wave functions. The minimization algorithm was chosen the Broyden-Fletcher-Goldfarb-Shanno (BFGS) scheme.²⁴ Its convergence criteria were set as follows: the force on the atoms were less than 0.03 eV/Å, the stress on the atoms were less than 0.05 GPa, the atomic displacement was less than 1×10^{-3} Å, and the energy change per atom was less than 1×10^{-5} eV. Based on the optimized crystal structure, the electronic structure and the optical properties were then calculated.

3. Results and discussions

3.1 Crystal structure

The five crystal structures of Si-O-N compounds are illustrated in Fig. 1. The coordination number of Si-O-N compounds is 4 for Si atoms, 3 for N atoms, and 2 for O atoms. α -quartz SiO_2 has a trigonal structure with space group of $P3_121$ (No 152) and local symmetry D_3^4 ; β -quartz SiO_2 has a hexagonal

structure with space group of $P6_222$ (№ 180) and local symmetry D_6^4 . Their structures are known to have rather regular or slightly distorted $[\text{SiO}_4]$ tetrahedron link together at the corners in forming a network structure. The difference between α -quartz SiO_2 and β -quartz SiO_2 is that the six-membered ring structure is different in these two crystal structure: the Si-O bonds are unequal with two types of bond lengths (1.6166 and 1.6194 Å) in α -quartz SiO_2 ; while the Si-O bonds are equal with bond length of 1.6144 Å in β -quartz SiO_2 . In the present work, the lattice constants of α -quartz SiO_2 are obtained as: $a = 4.9998$ Å, $c = 5.4934$ Å, which is very consistent with experimental measurement:²⁵ $a = 4.913$ Å, $c = 5.405$ Å; while the lattice constants of β -quartz SiO_2 are obtained as: $a = 5.0818$ Å, $c = 5.5668$ Å, which is very consistent with experimental measurement:²⁵ $a = 5.01$ Å, $c = 5.47$ Å.

$\text{Si}_2\text{N}_2\text{O}$ is the stable intermediate compound for the SiO_2 - Si_3N_4 compound system, resulting in its transition crystal structure between SiO_2 crystal structure and Si_3N_4 crystal structure. It has an orthorhombic structure with space group of $\text{Cmc}2_1$ (№ 36) and local symmetry C_{2v}^{12} . The tetrahedron of $[\text{SiN}_3\text{O}]$ is connected with each others via shared vertices. In $\text{Si}_2\text{N}_2\text{O}$ crystal structure, there three kinds of silicon atom ring structure: three-, four-, and six-membered ring. The three-membered ring is on the (100) plane, the four-membered ring is on the (011) plane, and the six-membered ring is on the (001) plane. The lattice constants of $\text{Si}_2\text{N}_2\text{O}$ are: $a = 8.932$ Å, $b = 5.525$ Å, $c = 4.870$ Å, which are very closely with experimental measurement:²⁶ $a=8.843$ Å, $b=5.473$ Å, $c=4.835$ Å.

α - Si_3N_4 has a trigonal structure with space group of $P31c$ (№ 159) and local symmetry C_{4v}^4 ; β - Si_3N_4 has a hexagonal structure with space group of $P6_3/m$ (№ 176) and local symmetry C_{6h}^2 . The tetrahedron of $[\text{SiN}_4]$ is connected with each others via shared vertices to form the three-dimensional network. There is only three-membered ring in the α - Si_3N_4 structure, while there are three- and four-membered rings in the β - Si_3N_4 structure. In the present work, the lattice constants of α - Si_3N_4 are obtained as: $a = b = 7.783$ Å, $c = 5.641$ Å, which is very consistent with previous calculated results:²⁷ $a = b = 7.766$ Å, $c = 5.615$ Å; while the lattice constants of β - Si_3N_4 are obtained as:²⁷ $a = b = 7.635$ Å, $c = 2.915$ Å, which is very consistent with previous calculated results: $a = b = 7.586$ Å, $c = 2.902$ Å.

All the crystal lattice parameters for these five Si-O-N compounds are tabulated in Table 1, which are well consistent with experimental data, indicating that the calculation methods in the present work are reasonable. Compared the crystal structures of α - SiO_2 and β - SiO_2 , one could find that the symmetry of

β -SiO₂ is higher than the symmetry of α -SiO₂, which is mainly exhibited by the rather regular [SiO₄] tetrahedron in α -SiO₂ structure and slightly distorted [SiO₄] tetrahedron in β -SiO₂ structure. The similar phenomenon could be found for α -Si₃N₄ and β -Si₃N₄: there are two different kinds of [SiN₄] tetrahedra in α -Si₃N₄ structure (in which every Si-O bond length or every N-Si-N bond angle is different from one another, implying the four nitrogen atoms are completely unequal); while only one kind of [SiN₄] tetrahedron in β -Si₃N₄ structure (in which two Si-O bonds are equal, and there are only two kinds of N-Si-N bond angle distribution). So, the symmetry of β -Si₃N₄ is higher than the symmetry of α -Si₃N₄. As the transition structure from SiO₂ to Si₃N₄, Si₂N₂O structure has lower symmetry, obviously distorted [SiN₃O] tetrahedron, and more complicated distribution of bond lengths or bond angles. The bond angle of Si-O-Si or Si-N-Si reflects the connection mode of tetrahedrons for these Si-O-N compounds. As shown in Table 1, there is only one connection mode between tetrahedrons in both SiO₂ structures, four connection modes between tetrahedrons in Si₂N₂O structure; eight connection modes between tetrahedrons in α -Si₃N₄ structure; three connection modes between tetrahedrons in β -Si₃N₄ structure. These crystal lattice parameters indicate that the symmetry of microstructure for atomic bonding in α -Si₃N₄ structure is very lower, although its macro-symmetry is higher than that of Si₂N₂O structure.

3.2 Electronic structure

The band structures of these five Si-O-N compounds are illustrated in Fig. 2. For α -SiO₂, the valence band maximum (VBM) is located at the K k-point, while the conduction band minimum (CBM) is located at the Γ k-point, which means α -SiO₂ is an indirect band gap semiconductor. The calculated band gap, the distance between VBM and CBM, is 8.702 eV, which is very consistent with experimental measurement ($E_g = \sim 8.7$ eV),²⁸ and larger and more accurate than that of previously reported band gap by theoretical calculations.^{27, 29} The band gap of β -SiO₂ (8.562 eV) is smaller than that of α -SiO₂, and also belongs to an indirect band gap semiconductor (the VBM is located at M k-point, while the CBM is located at the Γ k-point). In the present work, we found that the spin up states and the spin down states are completely coincident, owing to the pairing electrons in all these five Si-O-N compounds. Thus, for the band structure in Fig. 2, the lines of spin up states are completely overlapping on the lines of spin down states. In the case of Si₂N₂O, the VBM is located at the Γ k-point, as well as the CBM. So, the band gap of Si₂N₂O, 7.729 eV, belongs to the direct band gap. For α -Si₃N₄, the VBM is located at M k-point, while the CBM is

located at the Γ k-point. And the indirect band gap is 6.416 eV. In the case of β - Si_3N_4 , the VBM is located at the k-point of $\Gamma \rightarrow \text{A}$ line, while the CBM is located at the Γ k-point. And the indirect band gap is 6.160 eV. As shown in Table 2, the direct band gaps are slightly larger than the minimum band gaps as discussed above, except α - SiO_2 . This situation leads to difficult or certain confusion for the band gap measurement in the practice.

The parameters of band structure of these five Si-O-N compounds are listed in Table 2. From SiO_2 to $\text{Si}_2\text{N}_2\text{O}$ and to Si_3N_4 , as the oxygen component is gradually replaced by nitrogen component, the band gap (include the minimum band gap and the direct band gap at Γ k-point) is also gradually narrowing. The same or opposite variation tendency could be found for the band width variation of conduction band (CB) or valence band (VB). Because of the higher symmetry of β - SiO_2 structure, the O-2s states related band width is relatively concentrated. Based on the same reason, the N-2s states related band width is also relatively concentrated in β - Si_3N_4 structure. Another important parameter for optoelectronics applications is the effective mass of carriers on the top of VB or on the bottom of CB. In order to further compare the electronic properties of these Si-O-N compounds, the effective mass of holes on the top of VB and electrons on the bottom of CB along the different directions are calculated by fitting the extreme point of $E(k) \sim k$ relationship based on the band structures. The fitting results are illustrated in Table 3. The noticeable feature of the effective mass of carriers is anisotropic for all the five Si-O-N compounds. The minimum of hole effective mass for these five Si-O-N compounds is $0.198 m_0$ on A k-point along the direction of $[00\bar{1}] (\text{A} \rightarrow \Gamma)$ of β - SiO_2 structure, and the minimum of electron effective mass for these five Si-O-N compounds is $0.205 m_0$ on Γ k-point along the direction of $[001] (\Gamma \rightarrow \text{A})$ of β - Si_3N_4 structure. The present electronic structure and the corresponding parameters repeated the main features of Si-O-N compounds reported in previous literatures, but are more accurate than the earlier calculations.²⁷⁻³¹

In order analyze the chemical bonding information, the total and partial density of states (DOS) of these five Si-O-N compounds are plotted and compared in Fig. 3. In general, the peaks and features of DOS for these five Si-O-N compounds exhibit obvious similarity: (i) a deep band that is consisted by O-2s and/or N-2s states hybridized with Si-3s and Si-3p states; (ii) the lower and middle of VB is dominated by the hybridized states of O-2p and/or N-2p states with Si-3p states and S-3s states; (iii) the top of VB is dominated by the O-2p $_{\pi}$ or N-2p $_{\pi}$ nonbonding states; (iv) the CB is mainly contributed by the Si-3p states, and the bottom of CB shows the features of O-2p or N-2p with Si-3s, -3p bonding states. These bonding

features are in agreement with previously published experimental results.^{27, 29, 32} In addition to above mentioned similarities, due to the different microstructures, these five Si-O-N compounds also show some differences: (i) the O-2s related deep band in SiO₂ structures is rather sharp and concentrated, compared with the N-2s related deep band in Si₂N₂O and Si₃N₄ structures. In particular, the O-2s related deep band is separated with the N-2s related deep band; (ii) the VB of SiO₂ could be divided into three parts, while this phenomenon is not obvious in Si₂N₂O and Si₃N₄ structure; (iii) in the case Si₃N₄, there is a little energy band that is composed by N-2p states at the top of VB, especially in α -Si₃N₄ structure; (iv) the peaks at the bottom of CB are very weaker in both SiO₂ structure, resulting in the lesser occupied probability of electrons in the energy range. Because the Fermi energy level (E_F) is fixed at 0 eV in standard DFT calculations, so one could not directly observe the band shifting. However, the position of inner electronic states (such as O-2s or N-2s states) is relatively fixed at the certain energy range. Based on this principle, one could preliminary determine that nitrogen has higher energy levels compared with oxygen. And for the Si-O-N compounds, the top of VB is primarily formed by O-2p and/or N-2p states. Thus, the position of VBM is gradually shifting upward, when the oxygen atoms are replaced by nitrogen atoms (in other words, from SiO₂, to Si₂N₂O, and to Si₃N₄). At the same time, the bottom of CB is primarily formed by Si-3p states for all Si-O-N compounds, so the position of CBM is not shifting, when the oxygen atoms are replaced by nitrogen atoms. Just above reason, the band gap of Si-O-N compounds is gradually narrowing along with the increase of nitrogen content.

3.3 Optical properties

Fig. 4 illustrated the calculated dielectric function of five Si-O-N compounds. In the present work, the calculated values of the static dielectric constant ϵ_0 of α -SiO₂ is ~1.67, which is very smaller than that of experimental measurement (~4.5),³³ but is similar with previously reported theoretical calculated results.^{27, 29} The deviation between calculated results and experimental measurements maybe ascribe that only the straightforward electron transition from occupied states to unoccupied states is considered in DFT calculations. The calculated components of ϵ_0 for all Si-O-N compounds are listed in Table 3. Firstly, the value of ϵ_0 is increasing along with the increase of nitrogen content. Secondly, the ϵ_0 of β -SiO₂ is smaller than that of α -SiO₂. The same phenomenon could be observed in Si₃N₄ compounds. As discussed above, the symmetry of β -SiO₂ (or β -Si₃N₄) is higher than the symmetry of α -SiO₂ (or α -Si₃N₄). Based on this

calculated result, one could find that the optical properties not only are determined by the component of Si-O-N compounds, but also are determined by the microstructure of Si-O-N compounds. Thirdly, the intensity of dielectric function imaginary part is gradually becoming stronger along with the nitrogen content in the Si-O-N compounds. And the position of maximum of dielectric function (both real part and imaginary part) is gradually shifting toward lower-frequency range along with the nitrogen content in the Si-O-N compounds.

The refractive index curves of these five Si-O-N compounds are plotted in Fig.5. When the wavelength is smaller than 100 nm, the refractive index n is decreasing along with the N content; and then, the refractive index n is increasing along with the N impurity concentration. Finally, the refractive index n of α -SiO₂ is converged to ~ 1.292 , and the refractive index n of other Si-O-N compounds is respectively converged to ~ 1.273 (β -SiO₂), ~ 1.472 (Si₂N₂O), ~ 1.629 (α -Si₃N₄), and ~ 1.625 (β -Si₃N₄). There are two rules could be found: (i) the refractive index n is mainly determined by the proportion between oxygen and nitrogen in these five Si-O-N compounds, and is gradually increasing along with the nitrogen content; (ii) for the same Si-O-N compound, the refractive index n is slightly decreasing along with the increase of symmetry of crystal structure. For the refractive index k , namely extinction coefficient, the intensity is gradually increasing along with the increase of nitrogen content in these five Si-O-N compounds. At the same time, the band edge on the side of long wavelength is gradually red-shifting. The corresponding calculated reflectivity and absorption spectra of these five Si-O-N compounds are shown in Fig. 6. For these five Si-O-N compounds, the obvious light reflection is concentrated in range of 50~200 nm. When the wavelength is larger than 200 nm, the reflectivity of Si-O-N compounds is respectively converged toward a certain values: ~ 0.016 (α -SiO₂), ~ 0.014 (β -SiO₂), ~ 0.036 (Si₂N₂O), ~ 0.057 (α -Si₃N₄), and ~ 0.056 (β -Si₃N₄). This calculated result indicates that the visible-light reflection is enhanced as increasing nitrogen content, which is very worthy of attention if one used Si-O-N compounds films as anti-reflective layer. The light absorption properties of Si-O-N compounds are very similar with that of the refractive index k , as shown in Fig. 5: the light absorption in the range of 50~200 nm is gradually enhancing along with the increase of nitrogen content, and the absorption edge is also gradually red-shifting along with the increase of nitrogen content, owing to the narrowing of band gap and the enhancing electron occupied probability on the bottom of CB.

The optical properties of Si-O-N compounds are determined by their composition, crystal structure, and electronic structure. In turn, the differences of optical properties between these five Si-O-N compounds

could reflect the subtle differences between their crystal structure and electronic structure. Firstly, the N-related energy levels have relatively higher position, compared with O-related energy levels. So, the VBM of Si-O-N compound could be shifted upward by increasing nitrogen content, resulting in band gap narrowing. And then, the optical properties are varied by the increase of nitrogen content, including: the dielectric function constant, refractive index, reflectivity, absorption edge, and so on. Secondly, the different crystal structure (including: symmetry, connection mode of tetrahedrons, coordination number, etc.) leads to different atomic interaction. Thus, there are distinct chemical bond and electron distribution between atoms in different Si-O-N compounds. In Table 1, the average Mulliken population of atoms and bonds is also listed. For all the atoms (except Si atoms) and bonds, the populations exhibit the same increasing tendency along with the increase of nitrogen content in these five Si-O-N compounds. These calculated results indicate that the ionic interaction of Si atoms with O or N atoms is gradually weakening, while the covalent interaction of Si atoms with O or N atoms is gradually enhancing, from SiO_2 to $\text{Si}_2\text{N}_2\text{O}$ to Si_3N_4 . Just above intrinsic reasons to make the differences of optical properties of Si-O-N compounds. According to this principle, one could design novel Si-O-N compounds for specific optoelectronic applications, via controlling the composition and crystal structure.

4. Conclusions

The crystal structure, electronic structure, and optical properties of five Si-O-N compounds (including: α -quartz SiO_2 , β -quartz SiO_2 , $\text{Si}_2\text{N}_2\text{O}$, α - Si_3N_4 , β - Si_3N_4) have been calculated by DFT within GGA+U method. From SiO_2 to $\text{Si}_2\text{N}_2\text{O}$ and to Si_3N_4 , as the oxygen component is gradually replaced by nitrogen component, the band gap (include the minimum band gap and the direct band gap at Γ k-point) is also gradually narrowing, which is caused by upward shifting of valence band top that is composed by the O-2p _{π} and/or N-2p _{π} nonbonding states. The optical properties of Si-O-N compounds, including: the dielectric function constant, refractive index, reflectivity, absorption edge, and so on, are generally increasing along with the increase of nitrogen content. Furthermore, the microstructure of crystal in Si-O-N compounds also impact the detailed optical properties. In other words, the optical properties not only are determined by the component of Si-O-N compounds, but also are determined by the microstructure of Si-O-N compounds. These calculated results will be useful as reference data for analyzing the optical properties of more complicated SiO_xN_y compounds. According to this principle, one could design novel

Si-O-N compounds for specific optoelectronic applications, via controlling the composition and crystal structure.

Acknowledgements

The authors would like to acknowledge financial support from the National Natural Science Foundation of China (Grant No. U1037604).

References

1. O. W. Flörke, H. A. Graetsch, F. Brunk, L. Benda, S. Paschen, H. E. Bergna, W. O. Roberts, W. A. Welsh, C. Libanati, M. Ettlinger, D. Kerner, M. Maier, W. Meon, R. Schmoll, H. Gies and D. Schiffmann, in *Ullmann's Encyclopedia of Industrial Chemistry*, Wiley-VCH Verlag GmbH & Co. KGaA, 2000.
2. F. L. Riley, *J. Am. Ceram. Soc.*, 2000, **83**, 245.
3. M. E. Washburn, *Am. Ceram. Soc. Bull.*, 1967, **46**, 667.
4. W. Qiu, Y. M. Kang and L. L. Goddard, *Appl. Phys. Lett.*, 2010, **96**, 141116.
5. G. D. Wilk, R. M. Wallace and J. M. Anthony, *J. Appl. Phys.*, 2001, **89**, 5243.
6. P. Tung-Ming, L. Tan Fu and C. Tien Sheng, *Electron Device Letters, IEEE*, 2000, **21**, 378.
7. M. L. Green, E. P. Gusev, R. Degraeve and E. L. Garfunkel, *J. Appl. Phys.*, 2001, **90**, 2057.
8. R. Germann, H. W. M. Salemink, R. Beyeler, G. L. Bona, F. Horst, I. Massarek and B. J. Offrein, *J. Electrochem. Soc.*, 2000, **147**, 2237.
9. G. L. Bona, R. Germann and B. J. Offrein, *Ibm. J. Res. Dev.*, 2003, **47**, 239.
10. J. Weber, H. Bartzsch and P. Frach, *Appl. Optics.*, 2008, **47**, C288.
11. H. Dong, K. Chen, D. Wang, W. Li, Z. Ma, J. Xu and X. Huang, *physica status solidi (c)*, 2010, **7**, 828.
12. C. H. Chang, P. Yu and C. S. Yang, *Appl. Phys. Lett.*, 2009, **94**, 051114.
13. C.-H. Sun, P. Jiang and B. Jiang, *Appl. Phys. Lett.*, 2008, **92**, 061112.
14. D. Fischer, A. Curioni, S. Billeter and W. Andreoni, *Phys. Rev. Lett.*, 2004, **92**, 236405.
15. Q. Weibin, M. Yuhui, Z. Jing, W. Jia-xian, L. Mengke, L. Shiyan and P. Jiaoqing, *Jpn. J. Appl. Phys.*, 2014, **53**, 021501.
16. P. S. Peercy, *Nature*, 2000, **406**, 1023.
17. C. McGuinness, D. Fu, J. E. Downes, K. E. Smith, G. Hughes and J. Roche, *J. Appl. Phys.*, 2003, **94**, 3919.
18. R. K. Pandey, L. S. Patil, J. P. Bange, D. R. Patil, A. M. Mahajan, D. S. Patil and D. K. Gautam, *Opt. Mater.*, 2004, **25**, 1.
19. F. Rebib, E. Tomasella, M. Dubois, J. Cellier, T. Sauvage and M. Jacquet, *Thin Solid Films*, 2007, **515**, 3480.
20. F. Rebib, E. Tomasella, J. P. Gaston, C. Eypert, J. Cellier and M. Jacquet, *J. Phys.: Confer. Ser.*, 2008, **100**, 082033.
21. S. J. Clark, M. D. Segall, C. J. Pickard, P. J. Hasnip, M. J. Probert, K. Refson and M. C.

- Payne, Z. *Kristallogr.*, 2005, **220**, 567.
22. J. P. Perdew, A. Ruzsinszky, G. I. Csonka, O. A. Vydrov, G. E. Scuseria, L. A. Constantin, X. Zhou and K. Burke, *Phys. Rev. Lett.*, 2008, **100**, 136406.
23. V. I. Anisimov, J. Zaanen and O. K. Andersen, *Phys. Rev. B*, 1991, **44**, 943.
24. B. G. Pfrommer, M. Côté, S. G. Louie and M. L. Cohen, *J. Comput. Phys.*, 1997, **131**, 233.
25. R. W. G. Wyckoff and R. Wyckoff, *Crystal structures*, Interscience publishers New York, 1963.
26. C. Brosset and I. Idrestedt, *Nature*, 1964, **201**, 1211.
27. Y.-N. Xu and W. Y. Ching, *Phys. Rev. B*, 1995, **51**, 17379.
28. S. S. Nekrashevich and V. A. Gritsenko, *Phys. Solid State+*, 2014, **56**, 207.
29. Y.-N. Xu and W. Y. Ching, *Phys. Rev. B*, 1991, **44**, 11048.
30. P. Rulis, J. Chen, L. Ouyang, W.-Y. Ching, X. Su and S. Garofalini, *Phys. Rev. B*, 2005, **71**, 235317.
31. Y.-C. Ding, M. Chen, X.-Y. Gao and M.-H. Jiang, *Chinese Physics B*, 2012, **21**, 067101.
32. V. A. Gritsenko, J. B. Xu, R. W. M. Kwok, Y. H. Ng and I. H. Wilson, *Phys. Rev. Lett.*, 1998, **81**, 1054.
33. F. Gervais and B. Piriou, *Phys. Rev. B*, 1975, **11**, 3944.

Table 1. The lattice constants and parameters, and the atomic and bond average net charge from Mulliken’s population analysis of Si-O-N compounds in different crystal structures

		α -SiO ₂	β -SiO ₂	Si ₂ N ₂ O	α -Si ₃ N ₄	β -Si ₃ N ₄
		Trigonal	Hexagonal	Orthorhombic	Trigonal	Hexagonal
Symmetry		P3 ₁ 21 (D_3^4 , № 152)	P6 ₂ 22 (D_6^4 , № 180)	Cmc2 ₁ (C_{2v}^{12} , № 36)	P31c (C_{4v}^4 , № 159)	P6 ₃ /m (C_{6h}^2 , № 176)
Lattice Constant		a = b = 5.001 Å, c = 5.494 Å, $\alpha = \beta = 90^\circ$, $\gamma = 120^\circ$	a = b= 5.082 Å, c = 5.567 Å, $\alpha = \beta = 90^\circ$, $\gamma = 120^\circ$	a = 8.932 Å, b = 5.525 Å, c = 4.870 Å, $\alpha = \beta = \gamma = 90^\circ$	a = b = 7.783 Å, c = 5.641 Å, $\alpha = \beta = 90^\circ$, $\gamma = 120^\circ$	a = b= 7.635 Å, c = 2.915 Å, $\alpha = \beta = 90^\circ$, $\gamma = 120^\circ$
Crystal Volume /molecule.Å ³		39.6667	41.4997	60.0843	73.985	73.568
Density /g.cm ⁻³		2.515	2.404	2.769	3.149	3.166
Binding Energy / atom.eV		8.303	8.300	8.546	8.613	8.613
Bond Length /Å	Si-O	1.6165, 1.6194	1.6144	1.6295		
	Si-N			1.7272, 1.7293, 1.7351	1.7275, 1.7341, 1.7374, 1.7416; 1.7440, 1.7456,1.7504, 1.7556	1.7355, 1.7425, 1.7427
Bond Angle /degree	O-Si-O	109.154, 110.489	107.970, 109.843	108.233 ^a , 108.546 ^a		
	Si-O-Si	147.406	154.038	151.510		
	N-Si-N			107.415, 111.752	104.211, 108.710, 111.206, 112.905; 106.346, 108.710, 111.068, 114.372	108.009,110.259
	Si-N-Si			116.880, 118.695, 123.802	116.799; 117.254, 117.381, 122.859; 113.081, 120.255, 126.374; 119.999	113.542, 123.121; 120.000
	Si	2.35	2.37	1.99	1.81, 1.82	1.83
Net Change /e	O	-1.18	-1.18	-1.43		
	N			-1.12	-1.36, -1.38	-1.37, -1.38
	Si-O	0.53	0.53	0.56		
	Si-N			0.61, 0.67, 0.66	0.68, 0.67, 0.69, 0.68, 0.69, 0.67, 0.63, 0.65	0.62, 1.39, 0.58,

^a: this bond angle is of O-Si-N.

Table 2. The parameters of band structure of Si-O-N compounds in different crystal structures, the energy unit is eV.

	α -SiO ₂	β -SiO ₂	Si ₂ N ₂ O	α -Si ₃ N ₄	β -Si ₃ N ₄
Top of VB	K	M	Γ	M	$\Gamma \rightarrow A$
Bottom of CB	Γ	Γ	Γ	Γ	Γ
E _g (minimum) /eV	8.702	8.652	7.729	6.416	6.160
E _g (direct at Γ) /eV	9.167	8.791	7.729	6.486	6.292
VB width /eV	10.756	11.133	11.456	11.664	12.130
CB width /eV	10.730	10.574	9.585	9.572	9.320
O 2s-band-width /eV	2.150	2.011	~2.573		
N 2s-band-width /eV			~3.935	6.294	6.123

Table 3. The calculated effective mass of carriers, dielectric function constant, and refractive index along the different directions for Si-O-N compounds in different

crystal structures					
	α -SiO ₂	β -SiO ₂	Si ₂ N ₂ O	α -Si ₃ N ₄	β -Si ₃ N ₄
m_h^*/m_0	2.154 ($\Gamma \rightarrow A$: [001])	19.184 ($\Gamma \rightarrow A$: [001])	2.384 ($\Gamma \rightarrow Z$: [001])	0.439 ($\Gamma \rightarrow A$: [001])	1.914 ($\Gamma \rightarrow A$: [001])
	0.952 ($A \rightarrow \Gamma$: [00 $\bar{1}$])	0.198 ($A \rightarrow \Gamma$: [00 $\bar{1}$])	2.768 ($Y \rightarrow \Gamma$: [$\bar{1}\bar{1}0$])	0.426 ($H \rightarrow K$: [00 $\bar{1}$])	1.575 ($A \rightarrow \Gamma$: [00 $\bar{1}$])
	1.239 ($H \rightarrow K$: [00 $\bar{1}$])	1.334 ($H \rightarrow K$: [00 $\bar{1}$])	1.834 ($\Gamma \rightarrow S$: [010])	13.367 ($K \rightarrow \Gamma$: [$\bar{1}\bar{2}0$])	0.485 ($H \rightarrow K$: [00 $\bar{1}$])
	8.986 ($K \rightarrow \Gamma$: [$\bar{1}\bar{2}0$])	1.933 ($K \rightarrow \Gamma$: [$\bar{1}\bar{2}0$])	1.407 ($R \rightarrow Z$: [$0\bar{1}0$])	2.128 ($\Gamma \rightarrow M$: [010])	3.532 ($K \rightarrow \Gamma$: [$\bar{1}\bar{2}0$])
	2.780 ($\Gamma \rightarrow M$: [010])	2.857 ($\Gamma \rightarrow M$: [010])		0.484 ($M \rightarrow L$: [001])	4.852 ($\Gamma \rightarrow M$: [010])
	2.007 ($M \rightarrow L$: [001])	1.679 ($M \rightarrow L$: [001])			0.655 ($M \rightarrow L$: [001])
m_e^*/m_0	0.925 ($\Gamma \rightarrow A$: [001])	0.993 ($\Gamma \rightarrow A$: [001])	1.506 ($\Gamma \rightarrow Z$: [001])	0.790 ($\Gamma \rightarrow A$: [001])	0.205 ($\Gamma \rightarrow A$: [001])
	0.991 ($K \rightarrow \Gamma$: [$\bar{1}\bar{2}0$])	0.994 ($K \rightarrow \Gamma$: [$\bar{1}\bar{2}0$])	0.756 ($Y \rightarrow \Gamma$: [$\bar{1}\bar{1}0$])	1.063 ($K \rightarrow \Gamma$: [$\bar{1}\bar{2}0$])	1.172 ($K \rightarrow \Gamma$: [$\bar{1}\bar{2}0$])
	0.958 ($\Gamma \rightarrow M$: [010])	1.037 ($\Gamma \rightarrow M$: [010])	1.368 ($\Gamma \rightarrow S$: [010])	1.095 ($\Gamma \rightarrow M$: [010])	1.269 ($\Gamma \rightarrow M$: [010])
			1.087 ($R \rightarrow Z$: [$0\bar{1}0$])		
$\epsilon_1(0)$	[100]/[010]: 1.6674	[100]/[010]: 1.6225	[100]/[010]: 2.0958	[100]/[010]: 2.6680	[100]/[010]: 2.6366
	[001]:1.6696	[001]:1.6188	[001]:2.2460	[001]:2.6226	[001]:2.6485
n	[100]/[010]: 1.2913	[100]/[010]: 1.2738	[100]/[010]: 1.4478	[100]/[010]: 1.6335	[100]/[010]: 1.6239
	[001]:1.2922	[001]:1.2724	[001]:1.4987	[001]:1.6196	[001]:1.6276

Caption of Figures

Fig. 1 The crystal models of Si-O-N compounds in different crystal structures. The red balls represent oxygen atoms, the blue balls represent nitrogen atoms, and the gold balls represent silicon atoms.

Fig. 2 The calculated band structure of Si-O-N compounds in different crystal structures. The blue lines represent spin-up states, and the red lines represent spin-down states. Owing to the spin up states and the spin down states of these Si-O-N compounds are completely coincident, the blue lines of spin up states are completely overlapping on the red lines of spin down states.

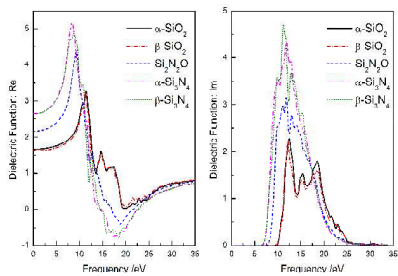
Fig. 3 The calculated total and partial density of state of Si-O-N compounds in different crystal structures.

Fig. 4 The calculated dielectric functions of Si-O-N compounds in different crystal structures

Fig. 5 The calculated refractive index of Si-O-N compounds in different crystal structures

Fig. 6 The calculated reflectivity and absorption spectra of Si-O-N compounds in different crystal structures

Graphic abstract



The optical properties of Si-O-N compounds are determined not only by their component, but also by their microstructure.

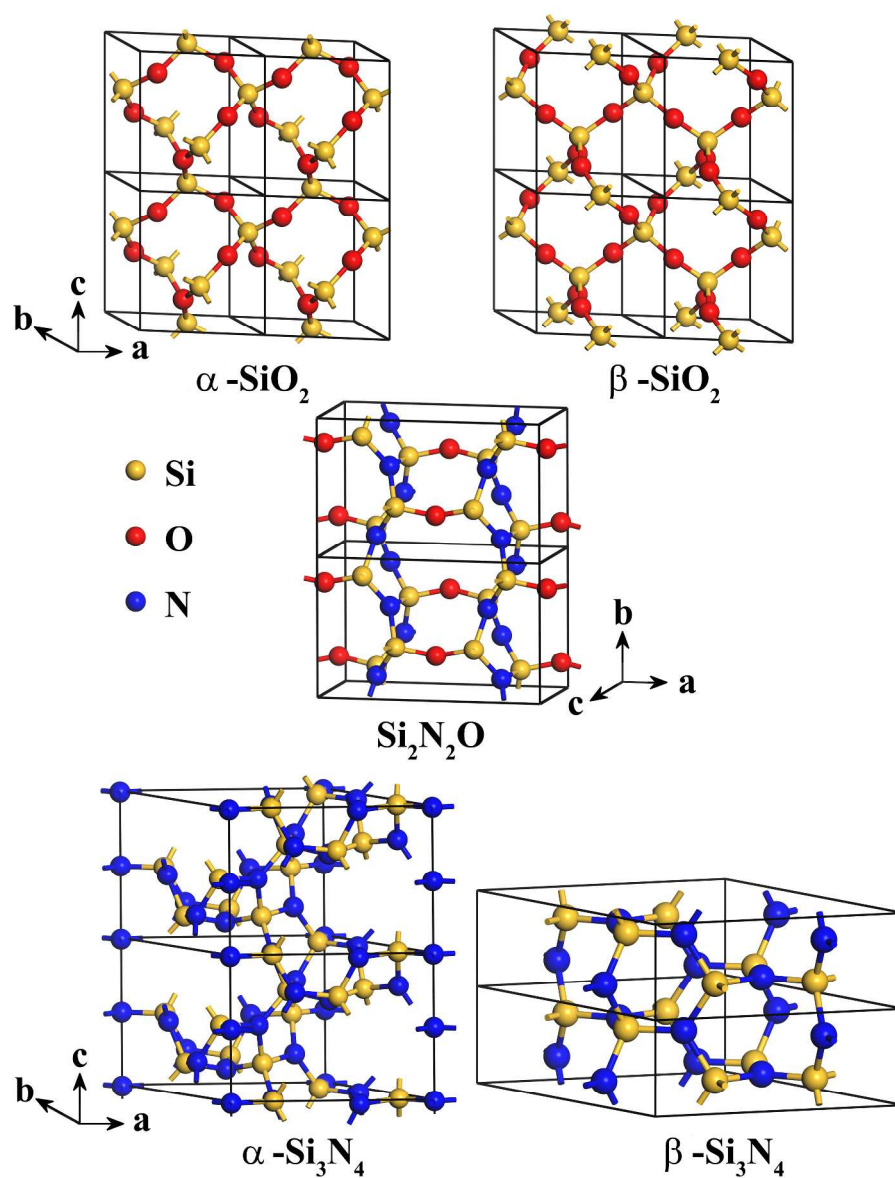


Fig. 1 The crystal models of Si-O-N compounds in different crystal structures. The red balls represent oxygen atoms, the blue balls represent nitrogen atoms, and the gold balls represent silicon atoms.
1047x1358mm (72 x 72 DPI)

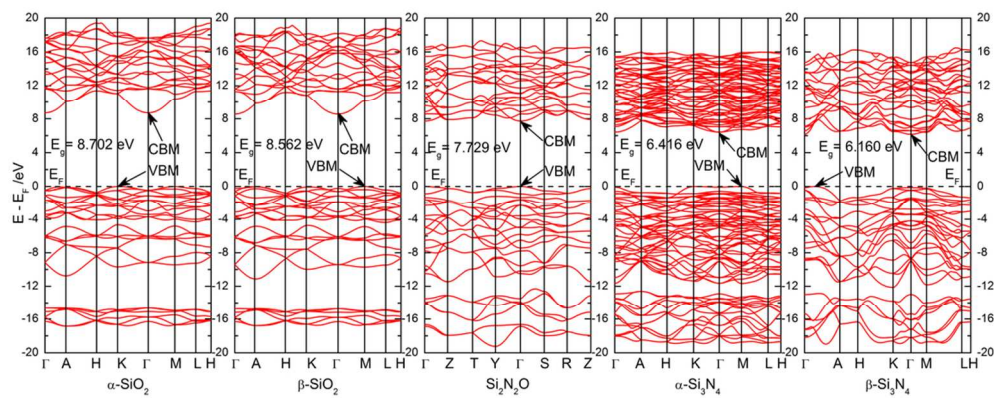


Fig. 2 The calculated band structure of Si-O-N compounds in different crystal structures. The blue lines represent spin-up states, and the red lines represent spin-down states.
98x40mm (300 x 300 DPI)

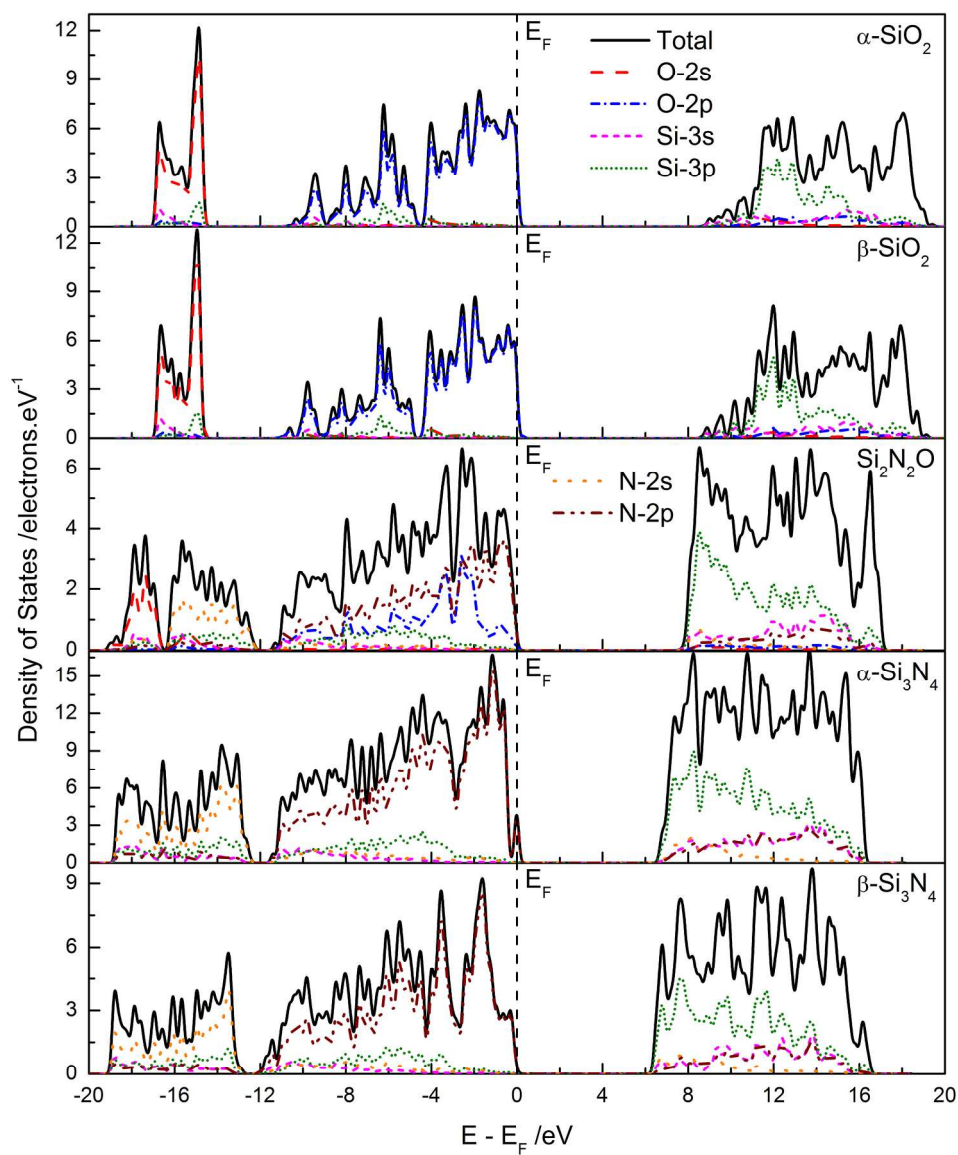


Fig. 3 The calculated total and partial density of stature of Si-O-N compounds in different crystal structures.
213x253mm (300 x 300 DPI)

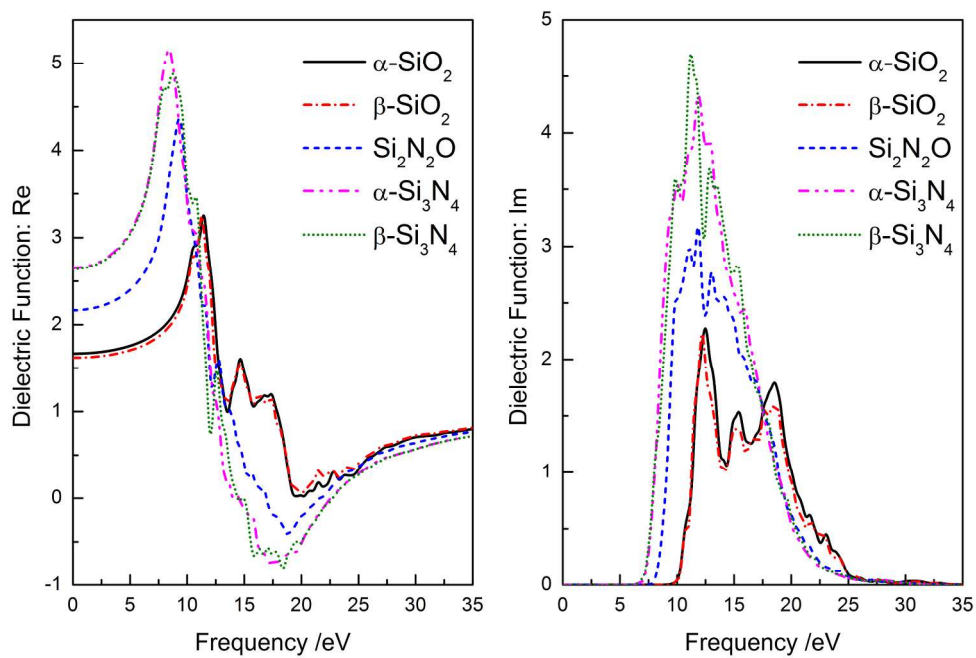


Fig. 4 The calculated dielectric functions of Si-O-N compounds in different crystal structures
209x148mm (300 x 300 DPI)

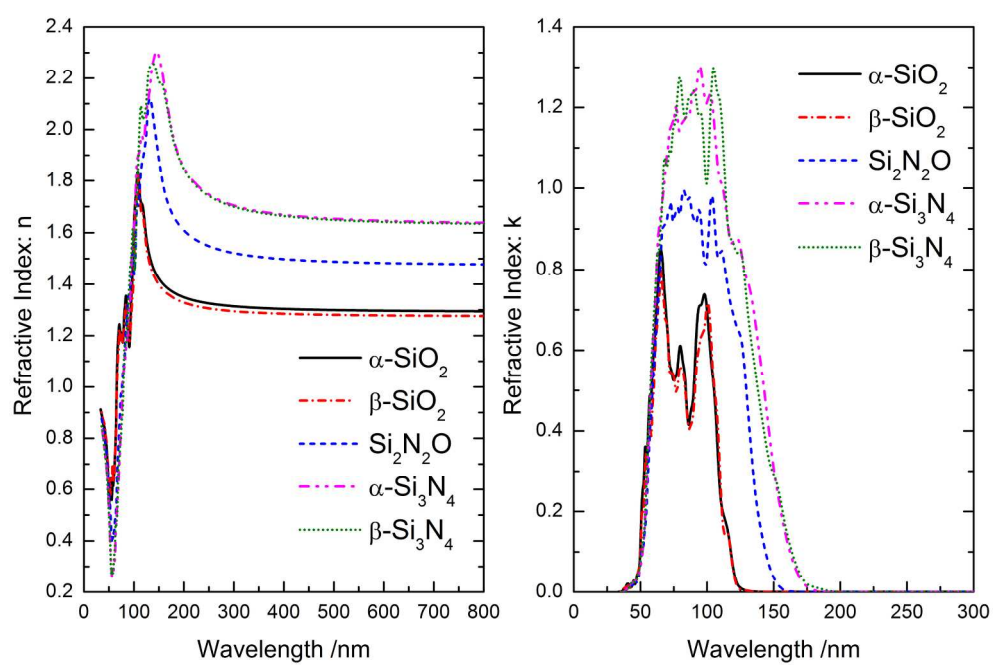


Fig. 5 The calculated refractive index of Si-O-N compounds in different crystal structures
209x148mm (300 x 300 DPI)

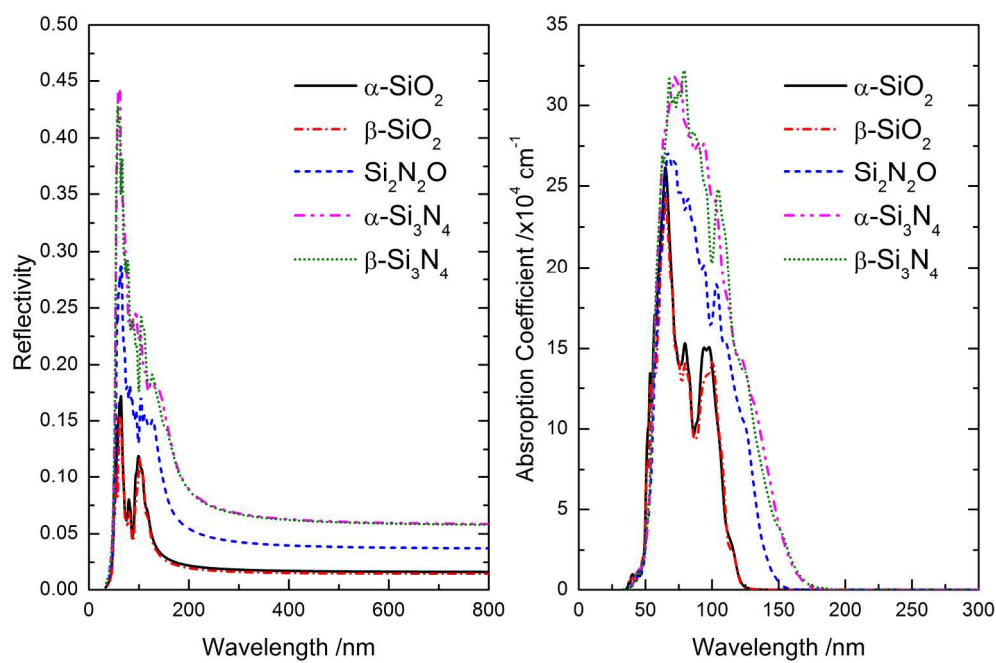


Fig. 6 The calculated reflectivity and absorption spectra of Si-O-N compounds in different crystal structures
209x148mm (300 x 300 DPI)